ChemPubSoc Europe

DOI: 10.1002/slct.201803114

Chemistry SELECT Full Papers

Electro, Physical & Theoretical Chemistry

Probing the Heterogeneity of Ionic Liquids in Solution through Phenol-Water Phase Behavior.

Abhineet Verma,[a] Namburi Eswara Prasad,[b] Jyoti Srivastava,[b] and Satyen Saha*[a]

Phenol-water system is important considering its resemblances to biological systems. Here, we explore this phenol-water system to get crucial information on ionic liquids (ILs). Comparative studies on the effect of high melting salts, micelles and ionic liquids (ILs) reveal interesting facts: while normal high melting salts such as KCl, CsCl and ionic surfactants (above and below critical micelle concentration (CMC)) show only an enhancement of critical solution temperature (CST) along with no substantial change in the shape of phase diagram, TX-100 shows an interesting trend. Below CMC, TX-100 shows normal trend while complete deviation is observed above CMC. When IL is added at various concentrations in the phenol-water system, the concentration-dependent effect on the phase diagram is observed. While at the low concentration, it follows the normal trend, at higher concentration phase diagram deviates drastically. The concentration at which this deviation is observed is termed here as Critical Ionic Liquid Aggregation Concentration (CILAC). Above CILAC, ILs exert an effect that resembles the effect of TX-100 micelles in the phenol-water phase diagram. Viscosity measurements of the system substantiate these data. Based on our observations, we propose that imidazolium chloride ILs constitute elliptical aggregates similar to TX-100 (having ~300 Å length) in solution above CILAC. To the best of our knowledge, this is the first report on the possible shape and size of ILs aggregation in solution.

Introduction

Phenol is a common chemical and a prototypical aromatic chromophore. Intermolecular interactions such as hydrogen bonding[1] in the phenol-water cluster are one of the interesting properties that can be examined by the study of phenol-water phase system.[2] This can provide some useful information like the interaction of the phenolic group with water, as -OH group of tyrosyl interaction with water in the human body. The hydrogen-bonded complexes of phenol are examples of interaction with aromatic acid, serving as a prototype for tyrosine residues in proteins interacting with water. Studies of phase behaviour can practically be simulated which helps us to understand the abnormal behaviour of the system, reflected clearly in its phase diagram.[3] Any change in the interaction between two components shows a variation in its phase behaviour.[4] which can also be mathematically expressed by Gibbs' phase rule (this rule applies to the non-reactive multicomponent heterogeneous system at thermodynamic equilibrium). Studies of these interactions between phenol and water may also be useful in drugs, polymers, and sensors.[5] As such intermolecular interactions are very important in understanding organic, organometallic, biomolecular structures, supramolecular assembly, crystal packing, reaction selectivity/specificity, and drug-receptor properties. In particular, the interaction of phenol with an interacting molecule is intriguing.[6] The phenol-water system is also a useful model for micro solvated phenol clusters.[7] The phenol-water/solvent potential-energy surfaces are found to be valuable for building model potentials in biomolecular simulations in the solvent environment. In addition to phenol-water,[8-9] phenol-ammonia is also reported.[9] There are interesting studies on the clusters of phenol-water and ammonia by various spectroscopic techniques[8,10] and by theoretical methods.[10] Very recently, the molecular mechanism of photo-acidity of phenol-ammonia has been elucidated.[11] Time dependent-DFT or ab initio calculations have greatly facilitated the interpretation of large spectroscopic data on phenol-water and phenol-ammonia.[12] The addition of the third component such as inorganic salts in the system found to play an interesting role.[13] Ionic liquids (ILs) have recently emerged as whole new materials much of which are yet to be discovered or understood.[14] ILs have found various potential applications; as powerful green solvents and catalyst,[15] electrically conducting fluids (i.e., electrolytes)[16] and in many other applications.[16] Ionic liquid is a substance that is composed solely of anions and cations and therefore must possess some kind of short-range organisation[17] (called charge ordering) to fulfil local electroneutrality condition and also to maximise the electrostatic interactions between ions of opposite sign. When looking at this kind of molecular architectures, microheterogeneity can be regarded as the important step in the understanding of the microscopic structure of these liquids. Therefore, it is no wonder that ILs must necessarily organise its high-charge density portions into local structures that obey electroneutrality. Soon after the

[a] A. Verma, Dr. S. Saha
Dept. of Chemistry, Institute of Science, Banaras Hindu University, Varanasi 221005, India
E-mail: satyen.saha@gmail.com
[b] Dr. N. E. Prasad, J. Srivastava
Defence Materials and Stores Research and Development Establishment (DMSRDE), Kanpur, India

Supporting information for this article is available on the WWW under https://doi.org/10.1002/slct.201803114

rediscovery of ILs a couple of decades back, a group of researchers have found considerable and significant pieces of evidence that there is a high degree of the organisation even in the fluid phase of room-temperature ionic liquids (RTILs).[18] It is believed that as a major consequence of their microscopic heterogeneity or nanostructure fluid character, ILs often show unique properties compared to their molecular liquid analogues. This nanoscale selforganization[19] is said to be the result of different types of interaction in the liquid phase, namely Columbic interaction and several weak interactions (such as van der Waals). A combined effect of all interactions eventually leads to the formation of nanostructured or microheterogeneity.[20] The possible existence of microscopic structural heterogeneity in pure ionic liquids has been suggested from both theoretical and experimental studies. Several groups, including ours, have been involved in research with ILs for understanding the bulk structure at a molecular level. With the help of state of the art Raman spectroscopic and X-ray crystallographic techniques, Hamaguchi and co-workers have obtained definite evidence for the existence of nano-structuredness in ILs.[21-22[Samanta and co-workers have also discussed the possibility of microheterogeneity based on the extensive fluorescence spectroscopic data.[22] Recently, we reported several pieces of 2D NMR and single crystal X-ray crystallographic experimental evidence, which indicate the existence of microscopic structural heterogeneity in ILs.[23] Also, we have observed that the nature of micro-heterogeneity does depend on the cation as evident from our comparative studies on imidazolium and piperidinium ILs.[24] We have obtained strong evidence that indicates that microheterogeneity in ILs is due to the crucial interplay of several types of weak interactions.[25]

Among many others, Canongia Lopes et al.,[26] Triolo et al.[19] and Voth et al.[18] have proposed the bicontinuous nature of ionic liquids through high-level molecular dynamics (MD) simulation. However, the issue of the existence of microheterogeneity is still under intense investigations as the consequence of microheterogeneity is far-reaching and will help us to explain much observation related to ILs behaviours and properties. In addition to pure IL system, there has been considerable interest generated recently to understand what happens to this heterogeneity of ILs when they are in solutions. The microscopic solvation environments in liquids are not well understood despite the fact that they critically determine the physical and chemical properties of liquids. Recently we have studied the microscopic solvation environments in prototype ILs using resonance Raman spectroscopy and molecular iodine and bromine as probe molecules.[27] Though not as extensive as for pure ILs, there are some reports in which the formation of self-aggregates,[22] micelles,[28] vesicles or layered like structures [25] are proposed when IL is dissolved in highly dielectric molecular solvent like water.

In this paper, we present most extensive studies of phenol-water phase behaviour at equilibrium in the presence of various high melting inorganic salts, surfactants (below and above CMC) and with dialkylimidazolium chloride ionic liquids (Figure 1) of different sizes at different concentrations. In addition to monitoring of miscibility temperatures at different

n=3	C_4mimCl
n=5	C_6mimCl
n=6	C_7mimCl
n=9	C_{10}mimCl

Figure 1. Chemical structures and corresponding codes of ILs used in this study.

compositions, we also studied the viscosity of solutions of various compositions. To the best of our knowledge, this is the first study of phenol-water phase behaviour with an aim to understand the influence of inorganic salts, surfactants and low melting organic salts (ILs). The effect of IL is found to be very interesting and helped us to determine the size and shape of the microheterogeneity of IL in solution.

Result and discussion

a) Methodology to construct the phase diagram:
i) Phenol-Water System

Pure phenol is crystalline at ambient temperature (melting point: 40.5 °C), and hence 80% phenol in water (4g colourless crystals of phenol was added in 1g triple distilled water) was prepared freshly to start the experiment of constructing phase diagram of the partially miscible phenol-water binary system. Since phenol was hygroscopic, weighing was done in a nitrogen atmosphere. This 80% phenol in water binary mixtures, which were colourless and transparent, was prepared in a hard-glass long test tube fitted with a thermometer (accuracy of $\pm$0.1 °C) and ring-end stirrer (made of aluminium/steel) as shown in Figure 2.

A burette was filled with tripled distilled water to add 0.5 mL of water (each addition) in aqueous phenolic solution to increase gradually the weight percentage (wt. %) of water in the system. To make the phase diagram independent of temperature, the x-axis of the phase diagram is plotted in wt. %. Since the densities of phenol (d = 1.09 g/cm^3) and water are close to 1, volume (in mL) and weight (in g) becomes interchangeable. This allows us to plot the phase diagram in "wt. % of phenol in the water" even though we take 0.5 mL water in each addition. The solution was stirred vigorously with the stirrer on each addition of water in phenolic solution. If the solution remains transparent at laboratory temperature, means that the system was at the homogeneous condition at that composition.

Further addition of water was necessary to get the system in heterogeneous condition. The appearance of milky or cloudy or opaqueness of the solution indicates the heterogeneous nature (shown in Figure 2-B). The solution is then heated in temperature-controlled water-bath to a temperature where the

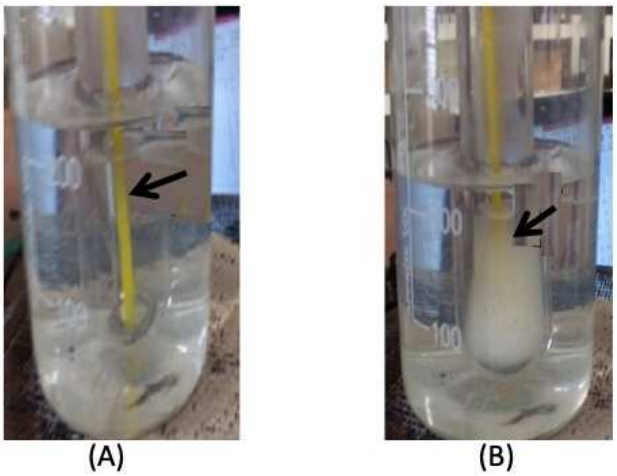

Figure 2. The glassware setup with thermometer and ring stirrer. (A)The hard glass test tube contains the transparent mixture of phenol-water indicating the homogeneous solution. (B) Shows the appearance of milkiness indicating heterogeneous phase. Arrow indicates the hard glass test tube having the mixture in a glass beaker.

milkiness disappears, and the solution becomes transparent. This temperature is noted as $T_{disappear}$. Hard-glass test tube was then removed from the hot-water-bath so that the milkiness reappears. The temperature at which it reappears is noted down as T reappear. The average of these two temperatures is plotted as "Average miscibility temperature / °C" on the y-axis. It is to be noted that $T_{reappear}$ provides better or closer reading to actual miscibility temperature. These steps are repeated with the addition of 0.5 mL of water until a complete phase diagram is obtained. Figure 3 shows the phase diagram of the pure phenol-water system obtained following the procedure described above.

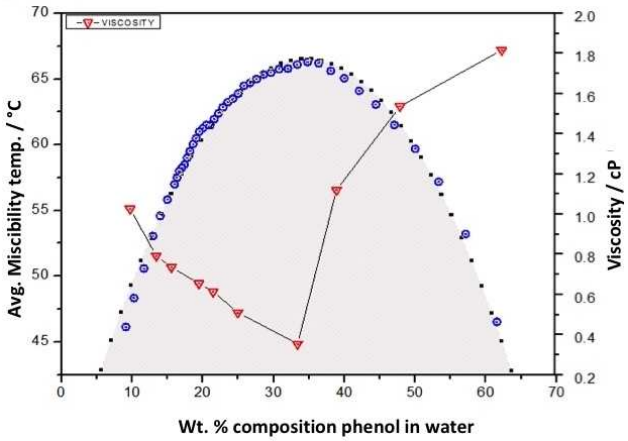

Figure 3. Phase Diagram of the phenol-water system. The black dotted line passing through the blue circled points is the best fit line represented by a polynomial of the second order, $y = 32.72 + 1.95x\text{-}0.0282x^2$. The black shaded area beneath the black dotted line indicates the heterogeneous phase while above the line indicates the homogeneity of the solution. The red triangle shaped point shows the corresponding viscosities at that percentage of the composition.

ii) Phenol-Water system with normal salts, micelles, and ILs:

The phase diagram of the phenol-water system having a third component was also determined following the same procedure described in the previous section with only one difference being that instead of pure water, we have added an aqueous solution of the third component in a definite concentration. The concentrations of the third component in water for the stock solution are kept such that after the addition of third component solution in aqueous phenolic solution, the concentration becomes definite x% (x = wt.% of phenol in water). These final concentrations are mentioned in the discussion. The miscibility temperature often decides the maximum concentration. In some cases, as low as 5% of KCl solutions, makes the maximum miscibility temperature (also known as Critical Solution Temperature (CST), described in preceding section) close to the boiling point of water and making the measurement impractical. Same experiments are done with the normal high melting salts (like KCl, CsCl), typical surfactant molecules (like CTAB, SDS, and TX-100) and finally with the well-known ILs (imidazolium cation based IL with variation in chain length in cation, such as C_4, C_6, C_7 and C_{10}).

b) Phase Behaviour of Phenol-Water System:

CST is a very important parameter in the phase diagram of the partially miscible binary system like phenol-water system. It is defined as the point (temperature) above which two immiscible liquids are completely miscible at any composition. Since the miscibility of phenol and water totally depends upon the temperature; the whole phase diagram is constructed by varying the composition and temperature as shown in Figure 3. CST of the phenol-water phase diagram is important concerning the fact that it often indicates the presence of a third component or impurity in general. The CST of the pure phenol-water system is found to be 66.3°C at 34.8 wt. % composition, which closely matches with the literature (66.8°C at 36.4 wt. %).[8,9,29] The shape of the phase diagram also looks the same as reported. We have also fitted the phased diagram we obtained with a polynomial equation (of order 2) to define the phase diagram better. This polynomial equation, $y = 32.72 + 1.95x\text{-}0.0282x2$ shall help one to get the phase diagram without even performing the experiment. Regarding the explanation of why the milkiness disappears with the increase of temperature, it can be explained considering the interplay of H-bonding interactions between these two components. On progressive addition of water in 80% phenolic solution, the H-bonding network among phenol molecules get disturbed, and heterogeneity appears as milkiness on increasing the temperature, the constituent molecular vibrations increase which helps to get the system back to homogeneous status. After a particular composition, 34.78 wt.%, further addition of water helps to build H-bonding network among water molecules in which phenol molecules are accommodated. This extensive H-bonded

network requires less amount of heat to accommodate further water, and therefore, the temperature required for homogeneity is less at higher phenol in water composition range (right part of the curve after CST).

H-bonding network among water molecules associated with phenol is also supported by theoretical calculation. ESI Figure S2 shows the calculated energies of various systems where the number of water molecules attached with phenol is increased systematically. The trend shows that with the increase in the hydrogen bonding the energy of the system decreases and is up to 5 membered planer ring structure cluster.[30] The cluster loses its planarity with the addition of further water molecule leading to destabilisation of the system. This theoretical study though done in gas phase clearly indicates that H-bonding association between water and phenol molecule has a definite role in stabilising the phenol-water system. David and co-workers have also demonstrated the existence of a π-hydrogen-bonded network structure for the phenol-water system through rigid-body diffusion quantum Monte Carlo calculation.[31-32] Our result corroborates very well with their finding that stable phenol-*x*water ($x \leq 4$) exists and beyond $x > 4$ leads to the unstable structure. Jacoby et al. have also found the same results as ours using ab initio calculations and termed the phenol-*x*Water ($x = 4$) as "book" structure.[30-33]

Since H-bonding interaction is expected to affect the viscosity of the solution, we have studied the viscosities of the system at various compositions (Figure 3). To the best of our knowledge, such in-depth studies of the phenol-water system have not been reported in the literature. We have observed a very interesting correlation between viscosity trends with that of the phenol-water phase diagram. Though both techniques are completely different, surprisingly they provide very similar data on critical composition at CST. The composition at CST as found from these two studies is 34.78 wt.%, (miscibility temperature measurement) and 34.78 wt.%, (viscosity measurement) respectively. This allows concluding that viscosity of the solution at critical composition is the least (here, 0.3 cp). This finding indicates that the critical composition of a phenol-water system can also be determined just by measurement of viscosity of the composition.[34] The viscosity is taken at a fixed temperature, here, in this case, 70°C as the CST of the system is found to be 66.3°C. It is clearly seen that if the miscibility temperature is high, then the corresponding viscosity of that composition is low and vice versa.[34-36] Thus, we can also use this measurement to check the composition of an unknown sample simply by measuring their viscosities.

c) Phenol-Water System with High Melting Salts: KCl & CsCl:

Effect of addition of a third component in the pure phenol-water system often shows up in the phase diagram. It has already been observed that the addition of inorganic salts like KCl raises the CST without any change in the shape of the phase diagram (Figure 4-A). The same is true for the addition of CsCl (Figure 4-B). In contrast, drop in CST is reported for the addition of compounds like urea or sucrose. The reason for enhancement or drop in CST is correlated with the solubility of

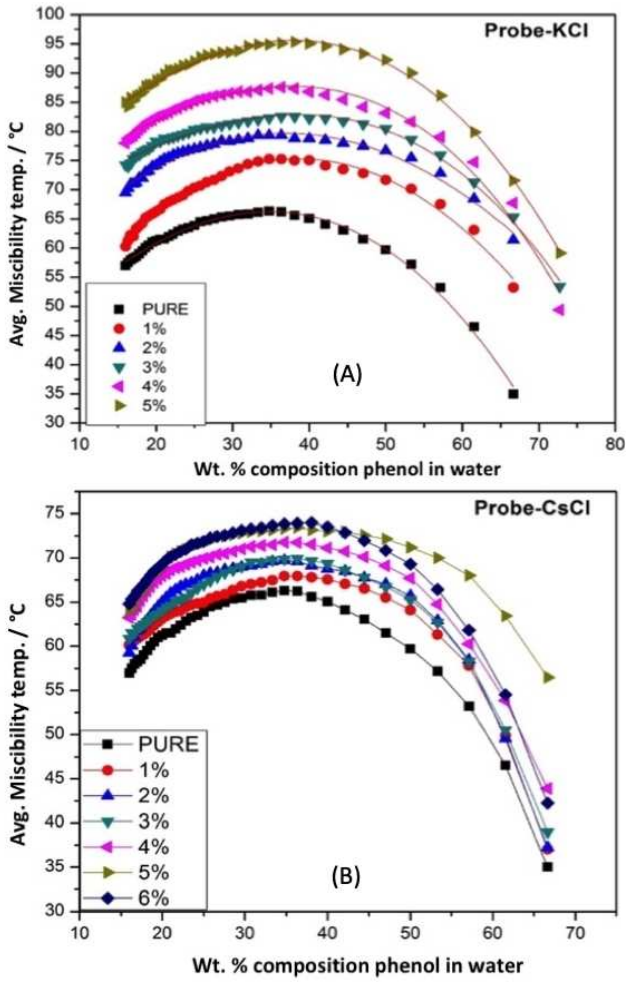

Figure 4. Phase diagrams of phenol-water systems having different concentrations of **(A)** KCl and **(B)** CsCl. Though there is no change in shape, enhancement of miscibility temperature on the successive addition is noteworthy. All data are given in **ESI Table S1**.

the third component in one or both the phases. If the component is soluble in both the phases, it is observed that CST decreases. In contrast, salts such as KCl and CsCl enhance the CST, as it is soluble only in the aqueous phase. A comparison of the effect of these two similar salts on CST of the phenol-water system reveals interesting facts. The enhancement is found to be profound in the case of KCl compared to the CsCl at the same concentration (Figure 5). KCl addition shows a significant temperature jump in CST on changing the concentration compared to CsCl. For example, CST of the system having 3% of KCl and CsCl are found to be 82.5 °C and 69.4°C respectively.

Detailed data of CST and compositions on the various amount of addition of salts are given in ESI Table S1. Since the anion component is the same in both the cases, the difference is expected due to either the size or charge density. However, their sizes do not vary significantly (ionic radius of Cs^+: 0.169 nm vs K^+: 0.133 nm). This finding stimulates us to investigate the size dependence of organic cation (of ionic liquids), which

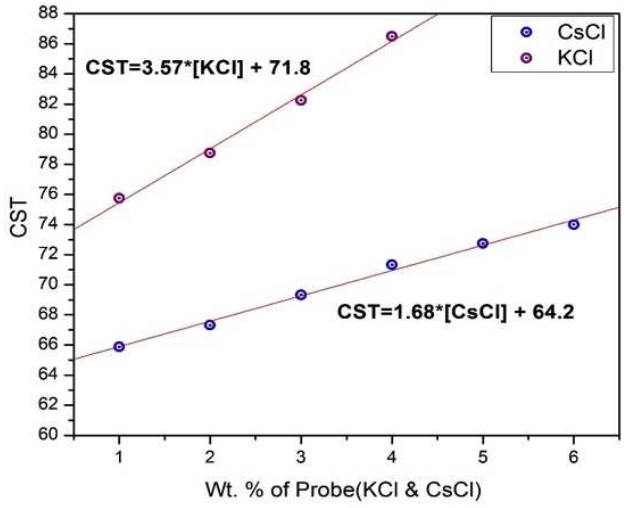

Figure 5. Variation of CST with the change of concentration of salts. The fitted lines show that CST varies linearly but with different magnitude of slopes. KCl has more influence than that of CsCl.

is discussed later. In addition to this size, another effect that can influence is the difference in solubility of KCl and CsCl at different temperatures. It is clear from the ESI Table S2 that solubility of these two salts are different at different temperatures and the trend is similar to the results we have observed. Also, this table also explains why there is a higher temperature jump for KCl solution compared to CsCl. The trend in the viscosity variation is found to be the same as that of pure one and is shown in ESI Figure S1. Therefore, it establishes that there is a correlation between viscosity, CST, and critical solution composition. If the miscibility temperature is more then corresponding viscosity is found to be less and vice versa. At the highest miscibility temperature, i.e., at CST, the viscosity is the minimum. The Figure S1 given in ESI has shown the phase diagram of KCl and CsCl with the corresponding viscosities data.

d) Phenol-Water System with Surfactant Molecules:

In the previous section, we have observed that the CST of a phenol-water system is sensitive to added salt and found to depend on the size/charge density of cation as well as solubility. Since there is no report in literature, we felt interested to explore this area by studying the effect of other types of molecules such as the surfactants. The surfactant can be ionic or nonionic. The ionic surfactant has hydrophobic and hydrophilic part joined together. The sources of hydrophobes are normally natural fats and oils, petroleum fractions, relatively short synthetic polymers, or relatively high molecular weight synthetic alcohols. However, the hydrophilic part gives the primary classification to surfactants: whether cationic, anionic or nonionic. While cationic hydrophiles are some form of an amine, the anionic hydrophiles are usually carboxylates (e.g., soaps), sulphates, sulphonates or phosphates. On the other hand, the nonionic hydrophiles are usually associated with polyethylene glycol chain. It is well-known that surfactant molecule makes 'micelle' above a certain concentration that is known as critical micellar concentration (CMC). The size and shape of micelle depend on the nature of constituents. ESI Figure S3 depicts pictorially several micelle types with their size and shape as reported in the literature.[37,38] While the hydrophilic end of the surfactant is strongly attracted to the water molecules, the force of attraction between the hydrophobe helps it to attain such shape in which both hydrophilic and hydrophobic regions coexist.

These surfactants, therefore give us the opportunity to study the effect of both homogeneous solution (below CMC) and heterogeneous solution (above CMC) on phase equilibria of phenol-water. Effect of these surfactants above and below their micellar concentration is studied here. Figure 6 depicts the change in phenol-water phase diagrams on the addition of various concentrations of different types of surfactants. While there is no appreciable change in shape or CST values on the addition of a cationic surfactant, CTAB solution (Figure 6-A) and anionic SDS solution (Figure 6-B, there is a slight change can be observed at conc. 100mM, but without any increase in miscibility temperature in lower conc.), there is an interesting shape change observed for TX-100 solution above CMC (Figure 6-C). When the concentration of TX-100 is significantly above CMC (such as 5 and 10 mM), the left side of the phenol-water phase diagram (below 40 wt% of phenol in water) deviates drastically. Instead of the normal decrease of miscibility temperature with an increase in water content, the miscibility temperature rises sharply. Since, below the CMC of TX-100, the shape and CST is the same, there is no effect of homogeneous surfactant solution on the phase behaviour of the phenol-water system. However, above CMC concentration, the shape of the curve changes, indicating the significant role of microheterogeneity of the micellar solution considering that above CMC, TX-100 forms well-know micelle (as depicted in Figure 6-C).

The micelles formed by CTAB and SDS above CMC are spherical in shape with the radius of 22.5 Å and 15.5 Å (Figure 6-A, B) respectively.[37] In contrast, the nonionic TX-100 have an elliptical shape with the major axis of 280 Å and the minor axis of 104 Å (Figure 6-C).[38] TX-100 has a hydrophilic polyethylene oxide chain (on average it has 9.5 ethylene oxide units) and an aromatic hydrocarbon lipophilic or hydrophobic group.[34] The hydrocarbon group is a 4-(1,1,3,3-tetramethylbutyl)-phenyl group. Undiluted TX-100 is a clear viscous fluid owing to the hydrogen bonding of its hydrophilic polyethylene oxide parts and has a viscosity of about 270 centipoise at 25 °C which comes down to about 80 centipoise at 50 °C.[37–38] Since TX-100 is quite different than CTAB and SDS, it is quite interesting to note the unique effect rendered by TX-100.

e) Phenol-water system with low melting salts (Ionic liquids) as the third component:

In the previous section, we have observed that the CST of the phenol-water system is sensitive to added salts, and micellar solutions. However, for a micellar solution, it is found that it

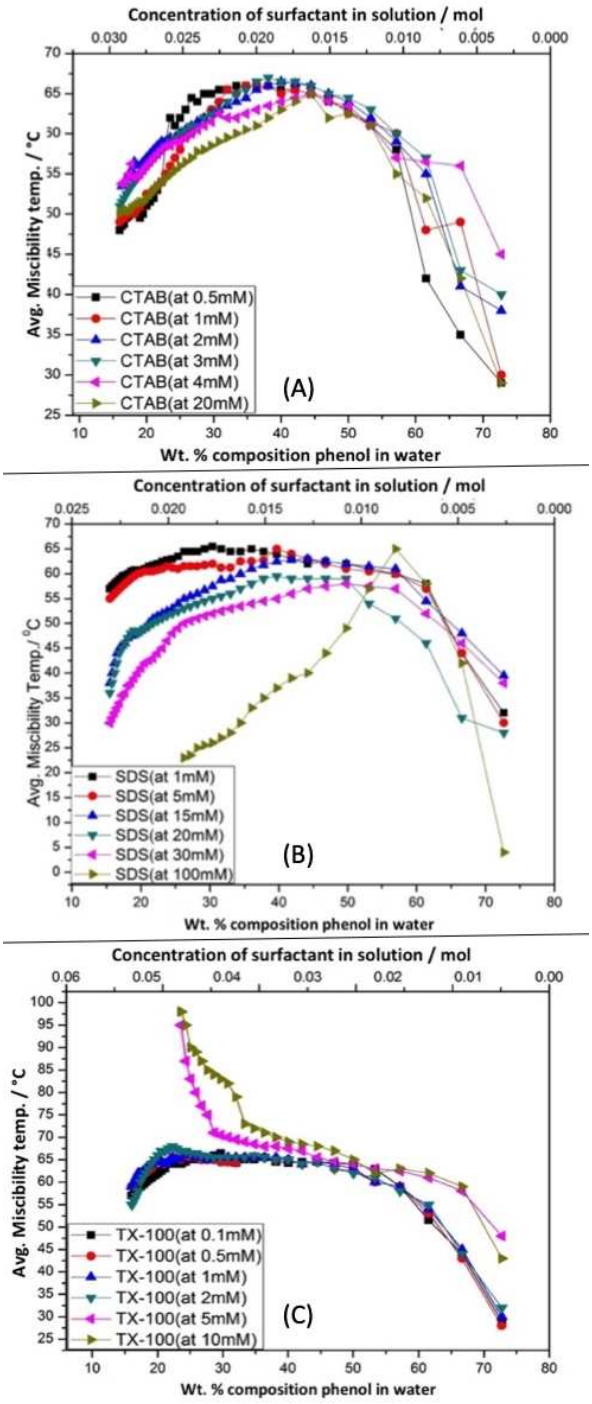

Figure 6. Phase diagram of phenol-water systems having different concentrations (above and below CMC) of surfactant molecules **(A)** CTAB and **(B)** SDS and **(C)** TX-100.

depends on the shape of the micelle, the constituent of the well-known micro heterogeneity. Since it is now well accepted that ILs is a new class of designer materials that are having micro-heterogeneity at the molecular level,[21,22] we felt interested to investigate the several with ILs. The advantage of choosing ILs is that one can alter the size of cation easily which is known to affect the micro heterogeneity[18] of ILs. Further, there are reports that ILs behaves like surfactants and form micelles above a certain concentration (termed as CMC of ILs).[18-20] However, we find it difficult to consider the micro-heterogeneity or aggregation simply same as that of micelles by the surfactant. As of now, there are no convincing reports which convey that ionic liquids in water form micelles which are identical to the microheterogeneity possessed by ionic liquids. If it was the same, the properties of ionic liquid solutions should have been the same as that of a micellar solution of surfactants, which is obviously not the case. Therefore, it is necessary to investigate without being biased and appreciate the uniqueness of ILs.

A series of dialkyl imidazolium cation based ILs have been synthesised to study the effect of the ILs (vide Figure 1). Cation size has been varied systematically. It is well accepted that ILs like surfactants possess two distinct regions, a polar hydrophilic and non-polar hydrophobic region and both of them are affected by cation size.[22] Therefore; the effect of the cation is discussed based on the size of the cation:

Ionic Liquid Cation size dependent study:

i) On the addition of C_4mimCl: C_4mimCl or n-butylmethylimidazolium chloride is one of the most popular ILs.[22,24] When 1 % solution of C_4mimCl is used in the phenol-water system, the resultant phase diagram shape is the same as that of the pure phenol-water system but shifted on the right side. Figure 7 shows phenol-water phase diagrams having a different amount of C_4mimCl. As the concentration of the ILs in the solution is increased from 1% to 2%, 3% and so on, the trend in the phase behaviour is same up to 50 wt.% Composition. However, after this composition, an unusual trend is noticed. Interestingly similar kind of trend is also seen for TX-100 above CMC, as discussed in the section. In addition to the shift of CST towards higher phenol composition, the normal trend of decrease in miscibility temperature on decreasing phenol wt. % composition disappears. The left side curvature of phenol-water almost disappears when 6% C_4mimCl is used as can be seen in Figure 7. The change in shape of the phase diagram is very systematic with the entire range of increase in wt. % of IL.

Figure 7 also shows the variation of viscosity of various phenol-water compositions when 1-4 wt.% C_4mimCl IL are used. At around 40 wt. % phenol in water, the viscosity of the solution is found to be maximum up to 3% C_4mimCl IL. At 4 wt.% IL, the viscosity drops drastically. This trend has a meaningful similarity with the Figure 9 where miscibility temperature is varied. We could not measure the viscosity of the phenol-water solution at higher wt. % of IL due to a practical problem with measurements. The movement of rolling ball is found to be hindered even though the solution looks quite homogeneous to the naked eye. These observations clearly indicate that after a certain concentration of IL in the phenol-water system, the system behaves very different. We would like to name this particular concentration of IL as "Critical Ionic Liquid Aggregation Concentration" or CILAC. We believe that above this CILAC, the constituent of IL come together to form aggregates. It is likely that there exist weak

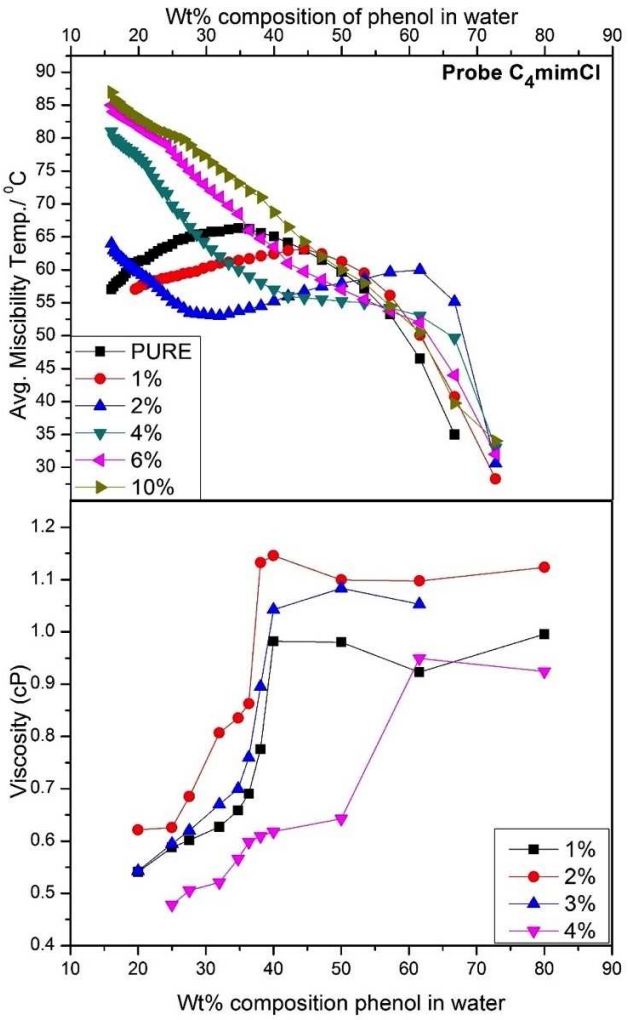

Figure 7. Top: Phase diagram of the phenol-water system having the various concentration of C_4mimCl as the third component. Bottom: Shows the viscosity of that composition at different wt. % composition of phenol in water.

interactions among aggregates and thereby constituting the overall micro- heterogeneity in IL.[22]

Aggregation behaviour of ILs in various solutions has been reported in some literature.[17-20] Overall, it appeases that for ILs, similar to surfactants, above a particular concentration, there is a change in solution properties, which closely resembles aggregations. The question follows: what is the size and shape of the aggregates? Though there are some recent reports[20] on the size of the aggregates or nanostructure domain, we have not come across any report on shape. Our studies indicate the most possible shape of the aggregates would be elliptical, i.e., similar to the shape of TX-100 micelle.

ii) On addition of CxmimCl (x = 6,7 and 10): Since the experiment with ILs C_4mimCl has provided new and interesting results, we have extended the work with other ILs having the same anion, mainly to validate our observation with C_4mimCl. Figure 8 shows the phase diagrams of phenol-water having different concentrations of ILs of various chain lengths. The chain length of the cation is varied from C_6 to C_{10} (Figure 8). In all cases, we can observe that the shape of the phase diagram is lost within an addition of 1% IL. However, when shorter chain length IL, i.e., e.g., C_4mimCl, the shape is preserved with 1% IL addition.

The loss of complete curvature is seen to appear faster (i.e., at a lower concentration) with a higher chain length of ILs. This indicates clearly that there is a correlation with the size of the ILs with the drastic change in phase behaviour. Viscosity measurements are found to be difficult with the phenol-water system with these higher chain lengths ILs. However, whatever viscosity data we could obtain indicate that there is a systematic change. The studies with various ILs also help us to understand that their two factors that affect the CILAC. One is obviously the concentration, and another one is the chain length or size of the ILs. Moving from C_4 to C_{10} we observed that if the chain length is smaller (as in case of C_4mimCl), the change in phase diagram does not appear at 1% solution (in a very similar manner as TX-100 do not alter the phase diagram below its CMC concentration). However, when the concentration of IL is increased to 2% the trend in phase diagram depicts similar behaviour as in the case of TX-100 above its CMC.

On the other hand, CTAB and SDS do not show any such change whether at below or above CMC. Thus this shows aggregation or nanostructure behaviour of IL is better correlated with TX-100. On further increase in the size of chain length (e.g., C_6mimCl) the similar trend in phase diagram as TX-100 is observed at 1% solution itself and on further increase in concentration to 2-5 % solution the trend is more prominent. Similarly, on increasing the chain length to C_7mimCl to C_{10}mimCl the same trend in the phase diagram of the phenol-water binary system is observed

In all the phase diagrams having added ILs, we can visualize the phase diagram composed of two regions, one within the ~40 wt% phenol in water and another above. The separation is very clear in pure phenol-water phase diagram (Figure 3) and is found to be at 34.8 wt.% (known as critical composition). However, with TX-100 or ILs added, after a certain concentration, this critical composition point starts disappearing. This disappearance is found to be correlated with the chain length of ILs. Figure 9 nicely depicts the effect of the size of the cations (at different concentrations), anion being unchanged. This figure also demonstrates that the loss of curvature appears faster with the higher chain length of ILs (e.g., while there is no loss of shape or curvature with 1 wt.% C_4mimCl, the clear and sharp rise is seen for C_{10}mimCl at the region of low phenol concentration with 1 wt.% itself). The details with numerical data of variation of CST with a change in mole fraction of water, phenol and added salts are given in ESI Table S4. The fit parameters of polynomial equation $y = ax^3 + bx^2 + cx + d$ used for various phase diagrams (where a, b, c are the coefficient and d is the intercept) are also included in the table. It is quite interesting to note that the moles of molecules, which are interacting at CST, are almost the same in all the cases.

Based on our results, we would like to propose that before a certain concentration of IL in the system, IL behaves more

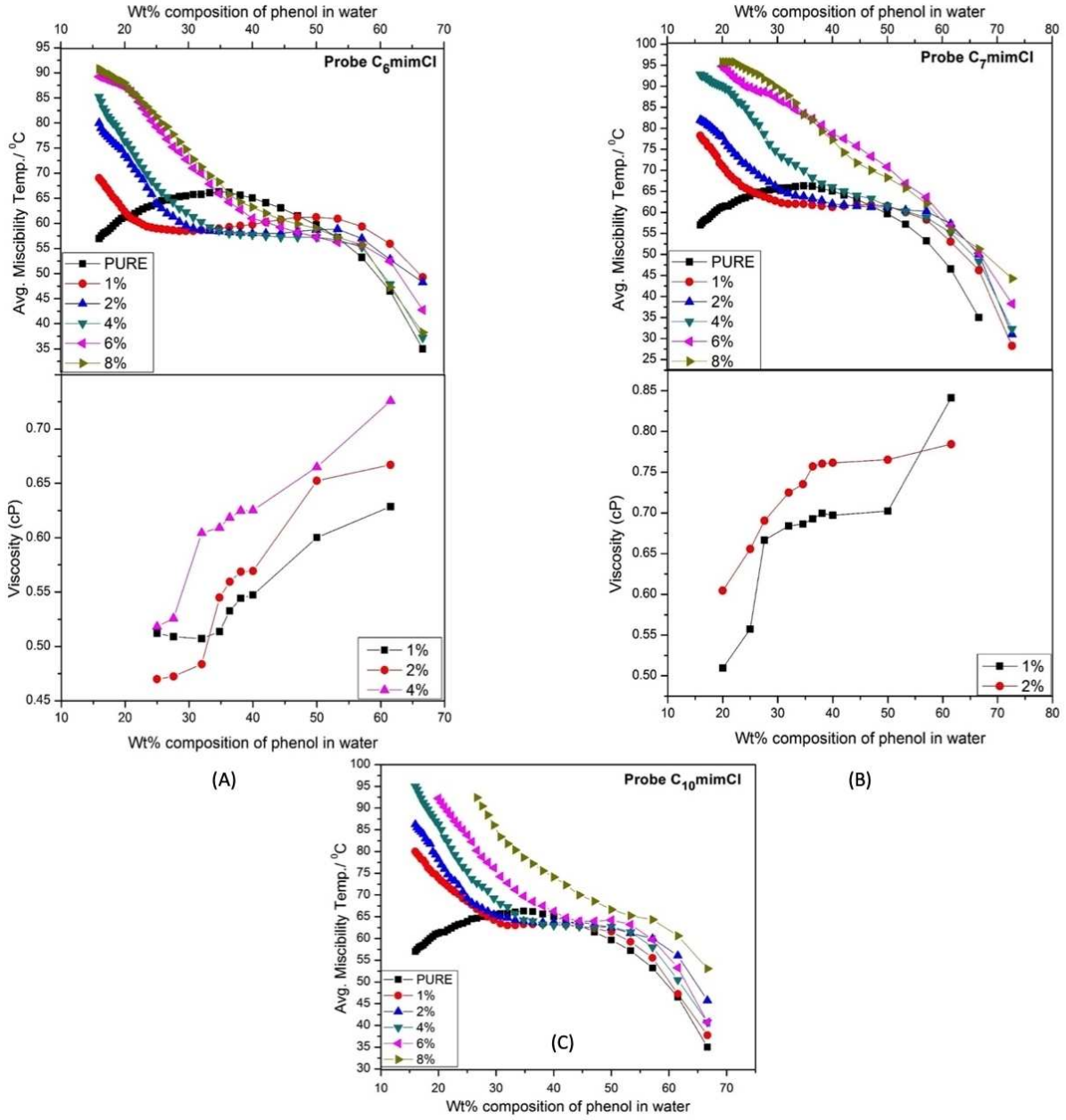

Figure 8. Phase diagrams of phenol-water systems having various concentrations of higher chain length containing ILs; (A) C_6mimCl, (B) C_7mimCl and (C) C_{10}mimCl.Variations of viscosities with compositions are also shown for systems containing C_6mimCl and C_7mimCl.

like normal salts. However, above that concentration, ILs behaves quite differently. That particular concentration is termed as CILAC. The value of CILAC depends on the size of the cation. Above this CILAC, IL behaves more like TX-100 micelle. Since above CMC, TX-100 is known to produce elliptical shape micelles; we propose that these dialkylimidazolium ILs above the CILAC produces microheterogeneity which is more like composed of elliptically shaped aggerates each having an approximate size of 300 Å. This possible scenario is presented pictorially in Figure 10.

We wish to mention here categorically that this estimation is purely based on the correlation with the well-established micelle formation surfactants as discussed. Since there are some practical problems like corrosiveness of the system and necessity of constant stirring of the mixture, we could not employ other size determining techniques like SAXS, SANS to verify the size but do hope that experts in these fields (SAXS and SANS) will investigate in the near future.

Conclusion

A series of experiments involving the construction of phase diagram of phenol-water partially miscible binary system at different conditions are reported here. In particular, the effect

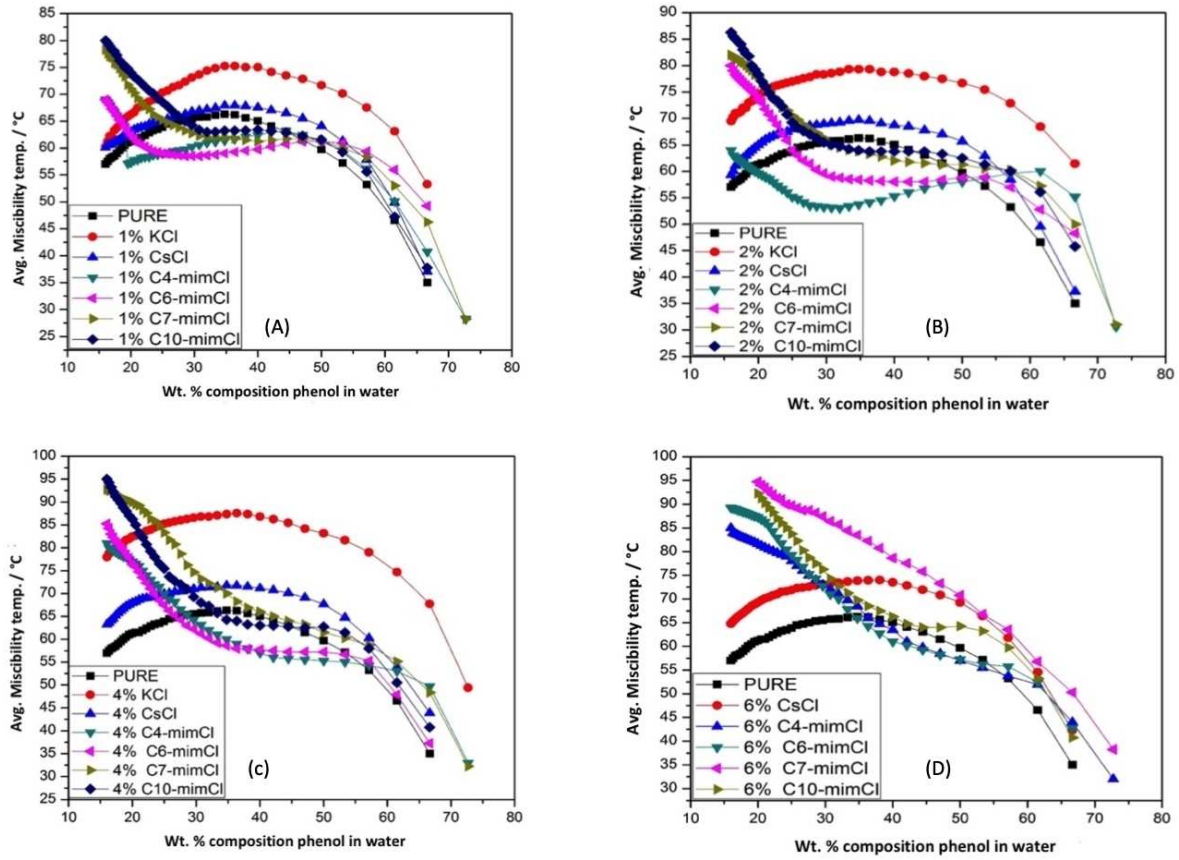

Figure 9. The above graph shows the phase diagram of phenol-water system having same concentrations of all the third components (KCl, CsCl, C_4mimCl, C_6mimCl, C_7mimCl, C_{10}mimCl). (A) 1% solution, (B) 2% solution, (C) 4% solution, (D) 6% solution.

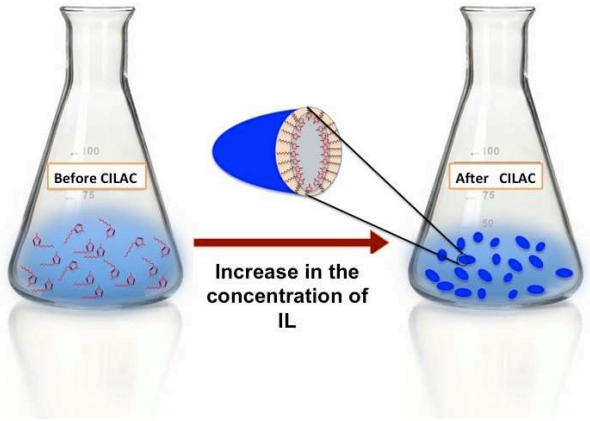

Figure 10. Schematic diagram showing the change in IL species influencing the phase diagram of the phenol-water system. Change of concentration of IL to form **CILAC** after a particular concentration.

of various salts (including ILs) on the shape and CST of phase diagram have been studied. While the normal high melting salts (such as KCl and CsCl) show a trend of simple increase of CST without any gross change of size or shape, the low melting salts (i.e., ionic liquids) above a certain concentration exert drastic change in phase-diagram itself. Therefore, our experimental results show that there is a unique concentration barrier above, which IL behaves quite differently. This concentration is termed here as "Critical Ionic Liquid Concentration" or "CILAC". This CILAC interestingly varies with the size of the IL. Considering that binary solvent mixtures (of ILs and normal molecular solvents) often used in organic reactions, this information of CILAC might help a lot for deciding the concentration of IL as a catalyst in a reaction. Above this CILAC, IL can influence the reaction path uniquely yielding product, which is otherwise not possible. There are many reports in literature where ILs (used as solvent or catalyst) are seen to produce unexpected product or product with very high yield. Our conclusion may be helpful to explain those observations. Further, it is observed that the bigger the size of the cation, the effect is more prominent even at a lower concentration. Since the size of the cation is also projected to alter the size of the microheterogeneity or nanostructures of ILs, we proposed that this drastic change in the phase diagram of the phenol-water system above the CILAC concentration of ILs are due to the existence of microheterogeneity of ILs. The size and shape of the aggregation are determined here by comparing with TX-100 micelle results due to its unprecedented similarities. Since TX-100 micelle is well known to form elliptical shape micelle having a dimension of 300 Å in length, our studies indicate

that imidazolium chloride based ILs possibly form elliptical shape aggregates of similar size. There is a good number of literature published in recent times where experimental evidences of micro-heterogeneity in ILs or formations of aggregations by ILs are reported as discussed in introduction. However, to the best of our knowledge, this is the first report indicating the possible shape along with approximate size of the micro-heterogeneity or aggregate of n-alkylimidazolium chloride ILs is reported as determined from the comparative studies of the effect salts, surfactants and popular ILs on the phase diagram of phenol-water systems.

Supporting information summary

The materials, experimental sections, synthesis, instrumentation, quantum chemical calculation and tabulated experimental data along with the phase diagrams of phenol-water systems containing various other surfactants, salts, pictorial representations of size and shape of CTAB, SDS and TX-100 surfactants are also given in the supporting information.

Acknowledgement

SS and AV acknowledge DMSRDE, Kanpur, for a research grant (TR/0569/CARS101) and thank department of chemistry, Institute of Science, Banaras Hindu University for providing instrumental facilities and other infrastructures. AV acknowledges his lab mate Manish Tiwari for help with ionic liquids and thanks to Mr. Manoj Kumar, Mr. Jagdish Srivastav & Mr. Abhinav Bharadwaj of B.Sc. laboratory for cooperation during the experiments.

Conflict of Interest

The authors declare no conflict of interest.

Keywords: CILAC · Ionic Liquids · Micro-heterogeneity · Phenol-Water · Shape- Size

[1] R. Parthasarathi, V. Sathyamurthy, N. Sathyamurthy, *J. Phys. Chem. A* **2005**, *109*, 843–850.
[2] G. D. Peckham, I. J. McNaught, *J. Chem. Edu.* **2011**, *88*, 592–593.
[3] X. Xu, X. Wang, M. Wu, *J. Chem. Edu.* **2014**, *91*, 929–933.
[4] H. Wang, Z. Wang, L. Li, Y. Chen, *J. Chem. Eng. Data* **2016**, *61*, 1540–1546.
[5] A. N. Sekretaryova, A. V. Volkov, I. V. Zozoulenko, A. P. F. Turner, M. Yu. Vagin, M. Eriksson, *Anal. Chim. Acta* **2016**, *907*, 45–53.
[6] a) W. Hu, L. Ding, J. Cao, L. Liu, Y. Wei, Y. Fang, *ACS Appl. Mater. Interfaces* **2015**, *7*, 4728–4736; b) S. K. Panja, N. Dwivedi, H. Noothalapati, S. Shigeto, A. K. Sikder, A. Saha, S. S. Sunkari, S. Saha, *Phys. Chem. Chem. Phys.* **2015**, *17*, 18167–18177.
[7] A. Fujii, T. Ebata, N. Mikami, *J. Phys. Chem. A* **2002**, *106*, 8554–8560.
[8] R. M. Helm, H. P. Vogel, H. J. Neusser, *J. Chem. Phys.* **1998**, *108*, 4496–4504.
[9] I. Bandyopadhyay, H. M. Lee, K. S. Kim, *J. Phys. Chem. A* **2006**, *109*, 1720–1728.
[10] a) D. S. Ch. Janzen, W. Roth, K. Kleinermanns, *J. Chem. Phys.* **1999**, *110*, 11. b) N. Yamamoto, Y. Nishino, E. Miyoshi, *J. Chem. Phys* **2004**, *121*, 2058–2066.
[11] T. Shimizu, S. Yoshikawa, K. Hashimoto, M. Miyazaki, M. Fujii, *J. Phys. Chem. B* **2015**, *119*, 2415–2424.
[12] D. M. Benoit, D. C. Clary, *J. Phys. Chem. A* **2000**, *104*, 5590–5599.
[13] P. Gansen, D. Woermann, *J. Phys. Chem.* **1984**, *88*, 2655–2660.
[14] D. Swapnil, V. Mahesh, S. Diwakar, Y. C. Kyoo, W. Kailas, *Res. J. Chem. Environ* **2014**, *18*, 24–29.
[15] V. Ivanistsev, T. Mendez-Morales, R. M. Lynden-Bell, O. Cabeza, L. J. Gallego, L. M. Varela, M. V. Fedorov, *Phys Chem. Chem. Phys* **2016**, *18*, 1302–1310.
[16] E. J. Bieske', J. P. Maier, *Chem. Rev.* **1993**, *3*, 2603–2621.
[17] a) J. Łuczak, J. Hupka, J. Thöming, C. Jungnickel, *Colloids Surf. A Physicochem. Eng. Asp.* **2008**, *329*, 125–133. b) A. Triolo, O. Russina, R. Caminiti. H. Shirota, H. Lee, C. Santos, N. Murthy, E. Castner, *Chem. Comm.* **2012**, *48*, 4959.
[18] a) Y. Wang, G. A. Voth, *J. Am. Chem. Soc.* **2005**, *127*, 12192–12193. b) J. Araque, J. Hettige, C. Margulis, *J. Phys. Chem. B* **2015**, *119*, 12727–12740.
[19] a) A. Triolo, O. Russina, Hans-Jurgen Bleif, Emanuela Di Cola, *J. Phys. Chem. B* **2007**, *111*, 4641-4644. b) A. Triolo, O. Russina, B. Fazio, G. Appetecchi, M. Carewska, S. Passerini, *J. Chem. Phys.* **2009**, *130*, 164521.
[20] a) G. Inoue, Y. Shimoyama, Fe. Su, S. Takada, Y. Iwai, Y. Arai, *J. Chem. Eng. Data* **2007**, *52*, 98-101. b) B. Dong, X. Zhao, L. Zheng, J. Zhang, N. Li, T. Inoue, *Colloids Surf. A Physicochem. Eng. Asp.* **2008**, *317*, 666–672. c) S. Saha, H. –o. Hamaguchi, *J. Phys. Chem. B* **2006**, *110*, 2777–2781. d) H. -o. Hamaguchi, R. Ozawa, *Adv. Chem. Phys.* **2005**, *131*. e) T. Greaves, D. Kennedy, A. Weerawardena, N. Tse, N. Kirby, C. Drummond, *J. Phys. Chem. B* **2011**, *115*, 2055–2066.
[21] a) R. Ozawa, H. Hamaguchi, *Adv. Chem. Phys* **2005**, *131*, 85–104; b) S. Saha, S. Hayashi, A. Kobayashi, H. Hamaguchi, *Chem. Lett.* **2003**, *32*, 740–741; c) K. Iwata, H. Okajima, S. Saha, H. -o. Hamaguchi, *Acc. Chem. Res.* **2007**, *40*, 1174–1181; d) S. Saha, H. Okajima, O. Homma, H. –o. Hamaguchi, *Spectrochemica Acta: Part A* **2017**, *176*, 79–82; e) J. Dupont, P. A. Z. Suarez, *Phys. Chem. Chem. Phys.* **2006**, *8*, 2441–2452.
[22] a) D. C. Khara, J. P. Kumar, M. Mondal, A. Samanta, *J. Phys. Chem. B 117*, **2013**, 5156–5164; b) D. C. Khara, A. Samanta, *J. Phys. Chem. B* **2012**, *116*, 13430–13438.
[23] S. K. Panja, S. Saha, *Magn. Reson. Chem* **2017**.
[24] B. L. Bhargava, M. L. Klein, *J. Phys. Chem. A* **2009**, *113*, 1898–1904.
[25] K. Shimizu, M. Tariq, L. P. N. Rebelo, J. N. C. Lopes, *J. Mol. Liq.* **2010**, *153*, 52–56.
[26] K. Yoshida, K. Iwata, Y. Nishiyama, Y. Kimura, H. –o. Hamaguchi, *J. Chem. Phys.* **2012**, *136*, 104504.
[27] C. Jungnickel, J. Łuczak, J. Ranke, J. F. Fernández, A. Müller, J. Thöming, *Colloids Surf. A Physicochem. Eng. Asp.* **2008**, *316*, 278–284.
[28] a) M. Shukla, N. Srivastava, S. Saha, in *Ionic Liquids* (ed. S Handy), IntechOpen, London, **2011**, pp. **153–170**. b) M. Shukla, S. Saha, in *Ionic Liquids* (ed. Jun-ichi Kadokawa), IntechOpen, London, **2013**, pp. **61–84**.
[29] S. R. Y. Osamura, *J. Phys. Chem. A* **1998**, *102*, 14.
[30] P. Tarakeshwar, Kwang S. Kim. Djafari, K. Buchhold, B. Reimann, H.-D. Barth, B. Brutschy, *J. Chem. Phys.* **2001**, *114*, 4016–4024.
[31] W. R. Ch. Jacoby, M. Schmitt, Ch. Janzen, D. Spangenberg, K. Kleinermanns, *J. Phys. Chem. A* **1998**, *102*, 4471–4480.
[32] E. M. MasRobert Bukowski, K. Szalewicz , *J. Chem. Phys*. **2003**, *118*, 4386–4403.
[33] M. Baratpour, A. Karimipour, M. Afrand, S. Wongwises , *Int. Commu. Heat Mass Transfer* **2016**, *74* 108–113.
[34] M. Afrand, K. Nazari Najafabadi, M. Akbari, *Appl. Ther. Eng.* **2016**, *102*, 45–54.
[35] E. W. Barega, E. Zondervan, A. B. de Haan, *J. Chem. Thermodyn. Thermochem.* **2013**, *63*, 31–37.
[36] C. Carnero Ruiz, J. Aguiar, *Langmuir* **2000**, *16*, 7946–7953.
[37] G. Duplatre, M. F. Ferreira Marques, M. da Gracüa Miguel, *J. Phys. Chem.* **1996**, *100*, 16608–16612.
[38] J.-M. Chen, T.-M. Su, C. Y. Mou, *J. Phys. Chem.* **1986**, *90*, 2418–242.

Submitted: October 6, 2018
Accepted: December 10, 2018